CHAPTER VI

SIMULATION RESULTS AND VALIDATION OF MODEL

The present model is based on the DEM model developed by Y. Tsuji (1998). The particles are assumed to be spherical and monodisperse. The simulated results are compared with the experiment results and correlation of T. Kudra et. al. (1992) and M.I. Kalwar (1991).

6.1 Effect of aerodynamics on two-dimensional spouted bed with draft plates

6.1.1 Conditions of calculation

The geometry of the vessel is set as close as possible to the medium-scale experimental apparatus of Kudra (1992). As shown in Figure 6.1, the normal distance is the spacing between the draft plate and the slanting base. The particles are spherical and monodisperse. Their physical propertie are based on shelled corn, whose properties as well as the dimension of the vessel used in the present investigation and the experiments of Kudra(1992) and Kalwar(1991) are summarized in Table 6.1. The number of particles corresponding to the same bed height of 0.90 m as the experiments is approximately 26,000. The angle of the slanted base is 60 degrees. The friction coefficients (both static and kinetic) and the Poisson's ratio of the particles are 0.30 and 0.25, respectively. The coefficient of restitution is taken to be 0.90. The appropriate value of the spring constant at 800 N/m in the contact force model was determined in the same manner as Kawaguchi (1998). Air at 20°C and 1 atm is used as the fluid. The gas flow is two-dimensional.

The maximum allowable time step for numerical intergration is estimated using the oscillation period of the spring-mass system recommended by Tsuji et al.(1993).

$$\Delta t \leq \frac{\pi\sqrt{m/k}}{5} \tag{6.1}$$

where Δt and k are the integration time step and spring constant, respectively. The actual time step used is 0.0003 second. To determine the minimum spouting velocity, the superficial gas velocity is gradually reduced from a sufficient large

value. The superficial gas velocity is defined as the gas velocity over an empty cross section of the rectangular vessel. The calculation results will be verified against the experimental results of Kudra(1992) and Kalwar(1991).

Generally, a parabolic deflector is installed at the top of the 2DSB with draft plates in order to prevent the unintentional entrainment of particles and to enhance solids circulation by directing the particles from the spout back to both downcomers. Kalwar(1991) reported that the optimally installed deflector above the draft plates is centrally installed at a distance equal to 30% of the plate height. In the present simulation, no deflector is installed because the medium-scale experiment of Kudra (1991) does not use one. Nevertheless, the possible effect of a deflector will be estimated and discussed.

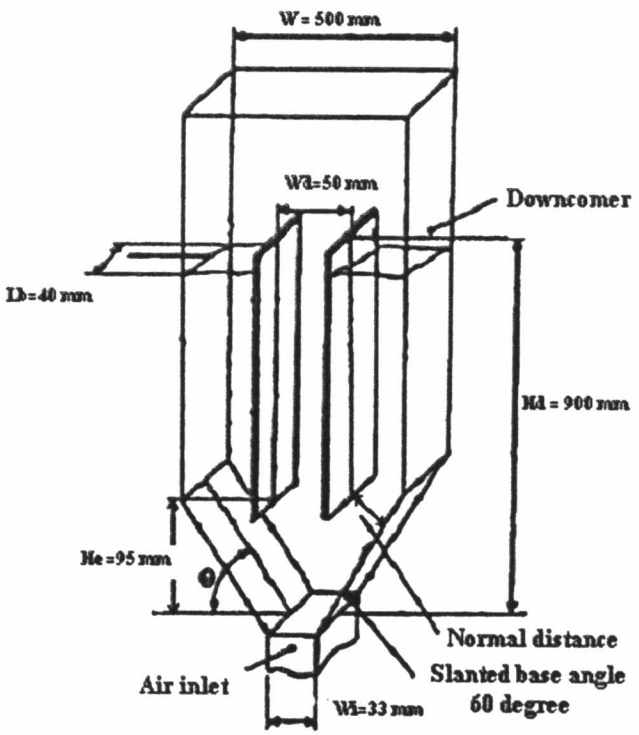

Figure 6.1 Schematics of the two-dimensional spouted bed

Table 6.1 Conditions of calculation and experiment (Kudra, 1992, Kalwar, 1991)

	Simulation	Experiment
Particle		
Diameter, d_p (m)	0.008	0.008
Density, ρ_p (kg/m^3)	1231	1231
Sphericity, ϕ	1	0.755
Vessel		
Width, W (m)	0.495	0.500
Depth, L_b (m)	0.40	0.040
Width of gas inlet, W_i (m)	0.033	0.033
Width of draft plates, W_d (m)	0.055	0.050
Separation height, He (m)	0.09538	0.100
Spout height, Hd (m)	0.912	0.900
Normal distance, (mm)	0.03797	0.04264
Slant angle, θ	60	60
Dimensionless		
W/W_i	15	15.1
W/d_p	61.8	62.5
Wi/d_p	4.1	4.1
Wd/W_i	1.6	1.5

6.1.2 Simulation results

In this section, the simulation results of aerodynamics in 2DSB with coefficient of friction 0.3, coefficient of restitution 0.9 and 26,000 particles are presented. The effect of separation height, coefficient of friction on particle circulation rate, the effect of draft plates and the effect of deflector also present in this section.

6.1.2.1 Minimum spouting velocity (u_{ms}) and pressure drop

Figure 6.2 shows the calculated pressure drop vs. the inlet gas velocity. As shown in Figure 6.2, the u_{ms} represents a turning point at which a slight reduction of the superficial gas velocity causes the spout to collapse and the pressure drop to significantly increase. Figure 6.3 shows some snapshots of the flow patterns in the spouted bed with draft plates. In Figure 6.2, the spout begins to collapse at the superficial gas velocity 1.25 m/s. The minimum spouting velocity and corresponding pressure drop can be estimated from the correlation given by Kudra (1992). The correlation of u_{ms} is as follows:

$$u_{ms} = \sqrt{gW_d}\,\phi^{0.68}\theta^{-0.084}\left(\frac{\rho_p - \rho_g}{\rho_g}\frac{H_e}{L_b}\right)^{0.15}\left(\frac{W_d d_p}{W_i H_b}\right) \qquad (6.2)$$

Our calculated minimum spouting velocity (u_{ms}) at bed height 0.9 m is 1.25 m/s while the prediction of Kudra's correlation is 1.18 m/s. The apparent discrepancy in the u_{ms} values may be ascribed to the slight differences in the vessel geometry. In the simulation H_e and W_d are 95 and 55 mm, respectively, whereas they are 100 and 50 mm in the experiment. Based on an experimental value of 1.18 m/s and equation (6.2), the predicted u_{ms} under the same vessel geometry should be $(1.18)(55/50)(95/100)^{0.15}$ = 1.29 m/s, which agrees very well with our simulation value of 1.25 m/s.

The correlation for the spouting pressure drop is as follows:

$$\Delta P_{ms} = \rho_b (gH_d)^{0.79}\theta^{0.33}\left(\frac{W_s}{W_b L_b \rho_b}\right)^{0.46}\left(\frac{s}{w_d}\right)^{0.42}\left(\frac{W_i H_b}{W_d H_d}\right)^{0.11} \qquad (6.3)$$

As in the experiment of Kalwar(1991), the pressure drop is measured between a central height of 11 mm above the bottom and the atmospheric pressure. The plotted pressure drop is time-smoothed over 1.8 seconds because slug flow causes the pressure to fluctuate strongly. Initially, the pressure drop increases as the superficial gas velocity increases. When the velocity reaches a certain value, the pressure drop starts to decrease gradually. Conversely, when the superficial gas velocity decreases from a sufficiently high value, the pressure drop gradually increases and then it increases significantly after passing the u_{ms} point. The hysteresis loop in the 2DSB occurs as shown in Figure 6.2 because the flow resistance of the dense packed bed is higher than the loose one. In practice, the hysteresis loop will be shrunk somewhat if the increase-decrease cycle is repeated by starting with a loose rather than a relatively dense packed bed. However, the hysteresis cannot be eliminated entirely due to the inherent irreversibility of the jet penetration phenomenon (Mathur and Epstein (1974)). The discrepancy between our calculated minimum spouting pressure drop and Kudra's prediction (1.40 vs. 1.20 kPa, or 1.16:1) can be attributed to the above difference in the predicted and experimental u_{ms} (1.25 vs. 1.18 m/s, or $(1.25/1.18)^2$ =1.12:1). It is assumed here that the pressure drop is proportional to the square of the velocity.

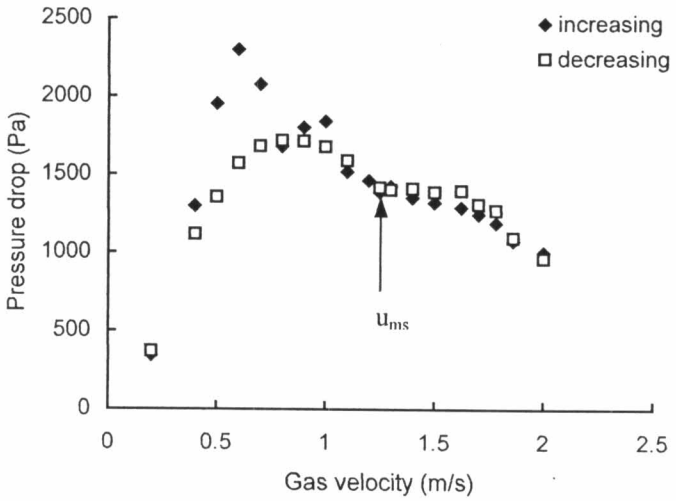

Figure 6.2 Gas velocity and calculated pressure drop with increasing and decreasing the gas velocity at bed height 0.9 m

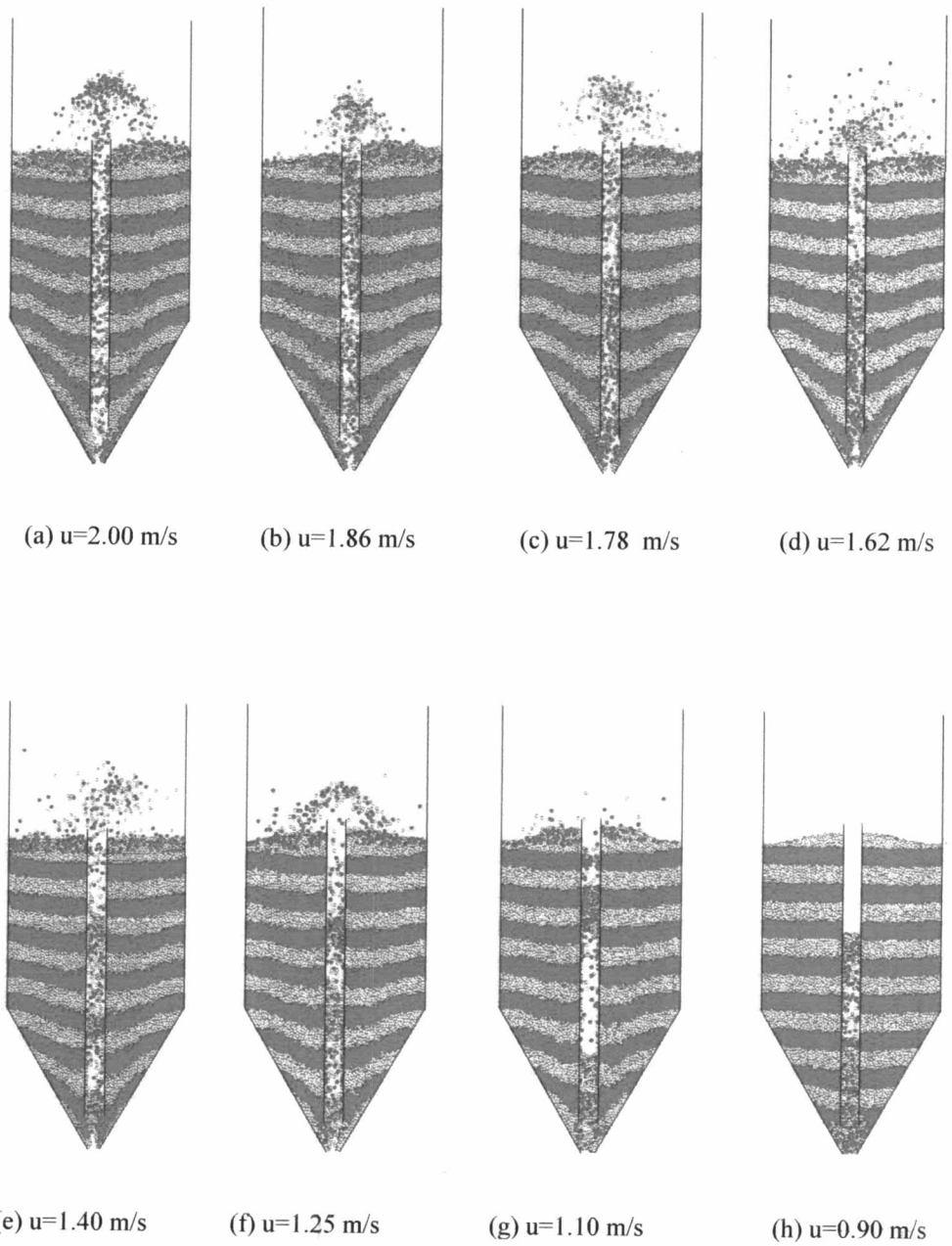

Figure 6.3 Flow patterns of 2DSBs with draft plates at 26,000 particles

6.1.2.2 Particle motion in the spout region

In this section, the spatial distribution of the particle velocity is investigated for each region: the spout and the downcomer. To save computer memory, the particle velocities are recorded every 0.03 seconds. The particle velocities are time-smoothed over a period of 1.8 seconds corresponding to 60 snapshots. Figure 6.4-6.8 show the profile of the time-smoothed vertical velocity of the particles at different heights in the spout region when the inlet superficial gas velocities are 1.25 m/s (= u_{ms}), 1.4 m/s (=1.12u_{ms}), 1.62 m/s (=1.30u_{ms}), 1.86 m/s (=1.48u_{ms}) and 2.00 m/s (=1.60u_{ms}). In this figure, z/R_d is the dimensionless height. The dimensionless distance (y/R_d) is measured from the central axis of the spout. The draft plate is located at $y/R_d = 1$. The particle vertical velocity in the spout decreases against the increased height because of slugging. The slugs formed in the upper region increase the flow resistance in the spout. The particle vertical velocities adjacent to the draft plates are lower than the local average value and some particles even fall down as shown in Figure 6.4. The height-averaged particle vertical velocity over the dimensionless height (z/R_d) 14.164 - 25.218 is shown in Figure 6.9 for various inlet superficial gas velocities. It is found that the height-averaged particle vertical velocities generally increase as the superficial gas velocity increases. In the present work, some slug flow occurs in the spout region at the minimum spouting velocity (u_{ms} = 1.25 m/s). The slugs gradually disappear when the superficial gas velocity further increases as shown in Figure 6.2. The fountain is stable at $u_i > 1.5\ u_{ms}$ (u_i > 1.86 m/s). The observed formation of slugs in the simulation of the 2DSB, which is related to the waves of particles developed in the lower region of the spout (Volpicelli(1967)), is consistent with reported experimental results. Formation of slugs is observed in the progressively incoherent spouting regime (Epstein(1987)). This regime occurs in the spouted bed when choking of the spout is the mechanism responsible for spout termination.

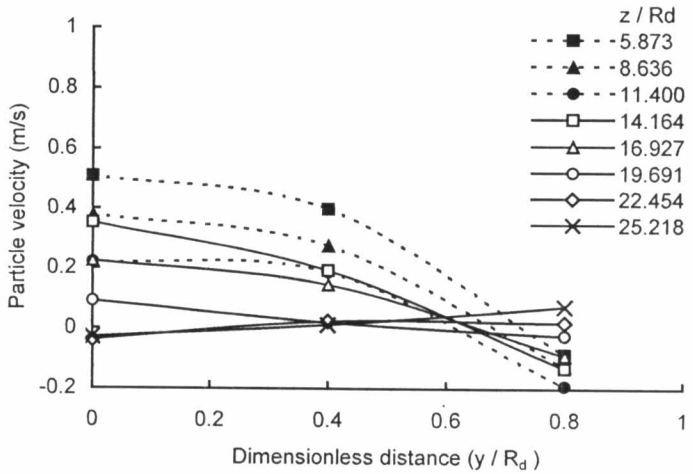

Figure 6.4 Particle velocity profile in the spout region at u_{ms} (1.25 m/s)

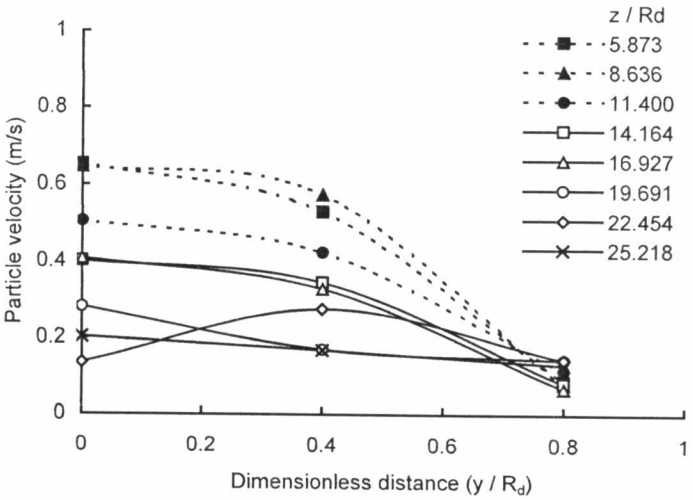

Figure 6.5 Particle velocity profile in the spout region at $1.12u_{ms}$ (1.4 m/s)

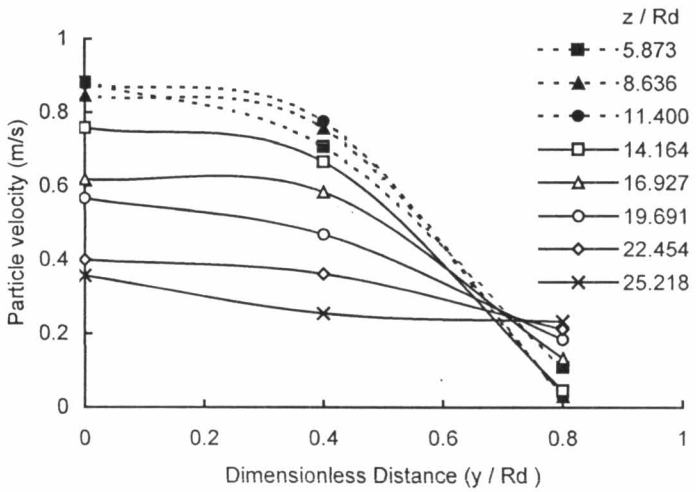

Figure 6.6 Particle velocity profile in the spout region at $1.30u_{ms}$ (1.62 m/s)

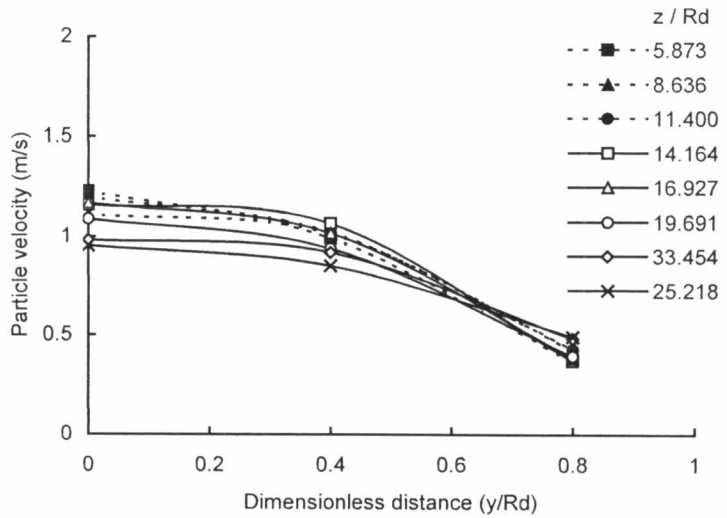

Figure 6.7 Particle velocity profile in the spout region at $1.48u_{ms}$ (1.86 m/s)

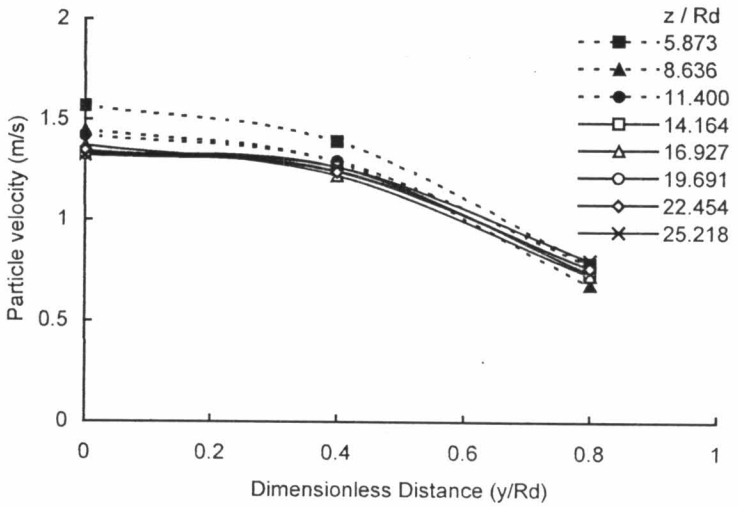

Figure 6.8 Particle velocity profile in the spout region at $1.60u_{ms}$ (2.00 m/s)

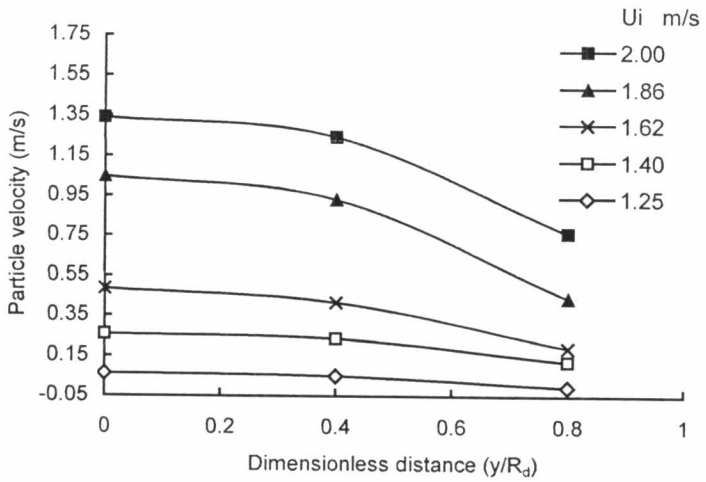

Figure 6.9 Average particle velocity profile at the dimensionless height (z / R_d) 14.164 – 25.218 in the spout region with various inlet superficial gas velocities

6.1.2.3 Particle motion in the downcomer region

The profiles of the particle vertical velocity with various inlet superficial velocities in the downcomer region are shown in Figure 6.10-6.14 for various heights. Here, downward particle velocities are plotted as positive values. The draft plate is located at $y/R_d = 1$ and the wall, at $y/R_d = 9$. As the height increases, the vertical particle velocities decrease in the vicinity of the draft plates whereas those near the vessel walls increase with the increasing height. Generally the particle vertical velocities near the walls are lower than those near the draft plates because the increased friction between the particles and the slanting base retards the return flow of the particles to the spout. In the lower region ($z/R_d = 5.873 - 11.400$), the particle vertical velocities are higher than in the upper region ($z/R_d = 14.164 - 25.218$) because of the reduction in the cross-sectional area by the slanting base. Figure 6.15 shows the profile of the height-averaged particle vertical velocity over the dimensionless height (z/R_d) 14.164-25.218 in the downcomer at various inlet superficial gas velocities. As expected, the particle velocities increase with the increasing superficial gas velocity. At the same height, the reduction in the particle downward velocity near the walls and near the draft plates can be attributed to the friction between the particles and the stationary walls and draft plates.

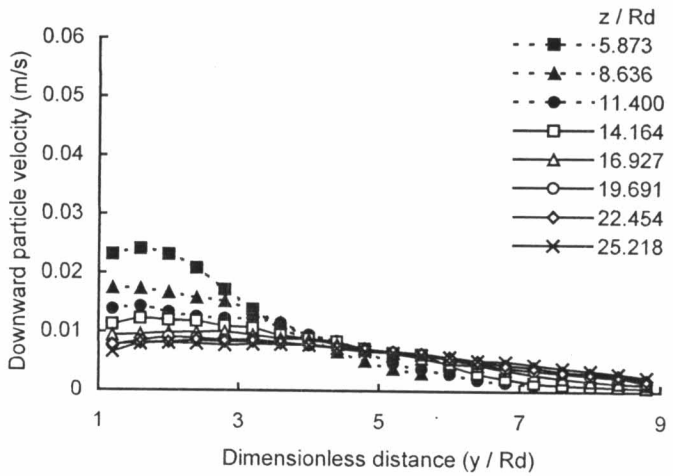

Figure 6.10 Particle vertical velocity profile in the downcomer for various dimensionless heights at superficial gas velocity at 1.25 m/s (u_{ms})

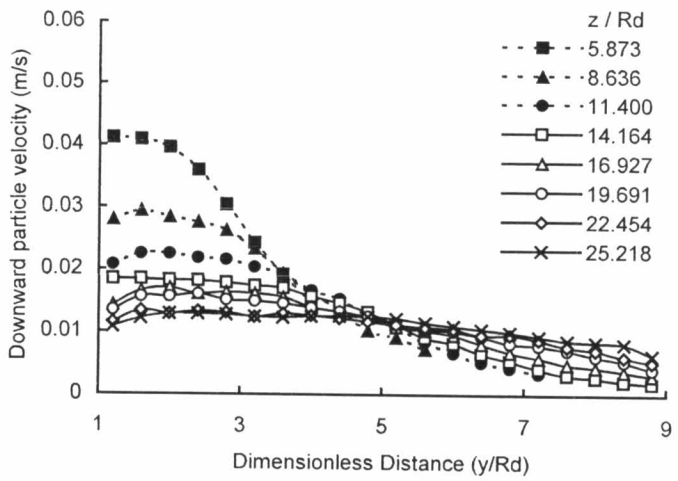

Figure 6.11 Particle vertical velocity profile in the downcomer for various dimensionless heights at superficial gas velocity at 1.12 u_{ms} (1.4 m/s)

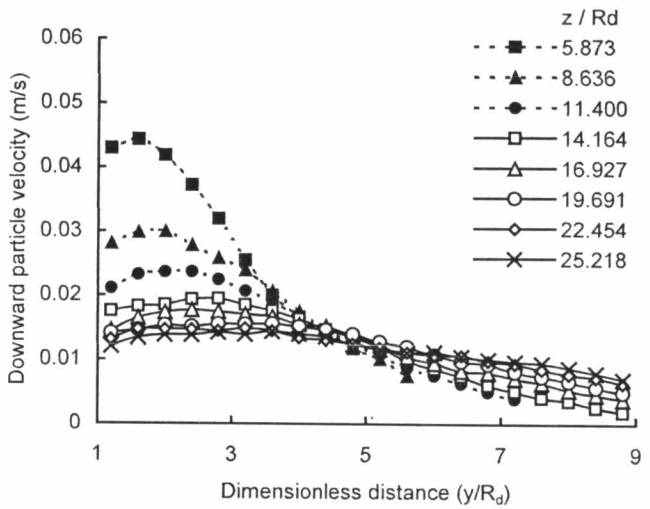

Figure 6.12 Particle vertical velocity profile in the downcomer for various dimensionless heights at superficial gas velocity at 1.30 u_{ms} (1.62 m/s)

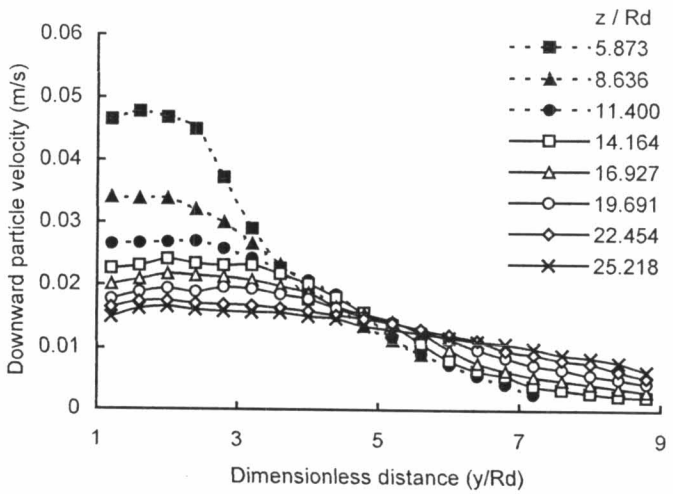

Figure 6.13 Particle vertical velocity profile in the downcomer for various dimensionless heights at superficial gas velocity at 1.48 u_{ms} (1.86 m/s)

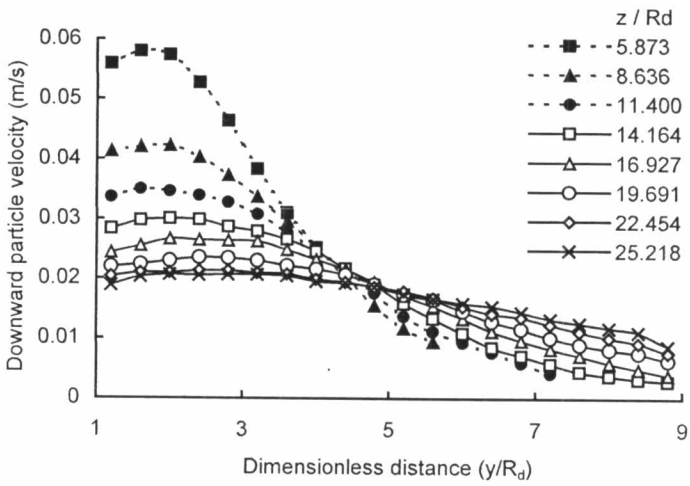

Figure 6.14 Particle vertical velocity profile in the downcomer for various dimensionless heights at superficial gas velocity at 1.60 u_{ms} (2.00 m/s)

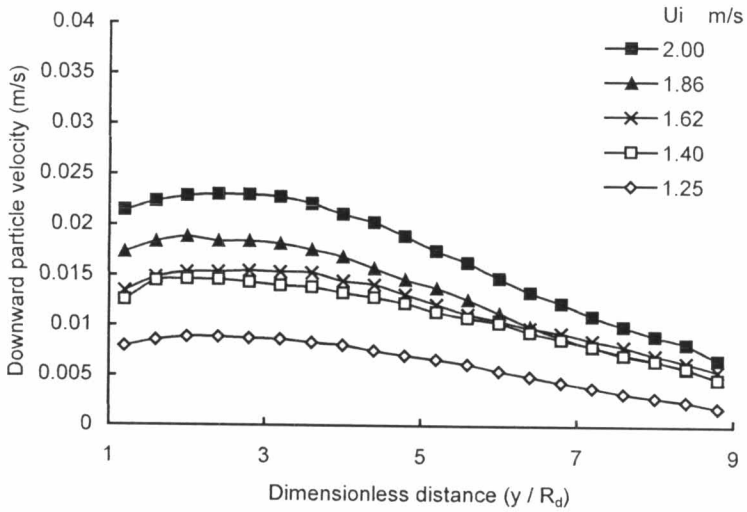

Figure 6.15 Profile of height-averaged particle vertical velocity over the dimensionless height (z/R_d) 14.164 - 25.218 in the downcomer at various inlet superficial gas velocities

6.1.2.4 Fluid motion in the spout and downcomer regions

The profiles of the height-averaged vertical fluid velocity over the dimensionless height (z/R_d) 14.164 - 25.218 in the spout region are shown in Figure 6.16 for various inlet superficial gas velocities. The calculated terminal velocity of the particles is 15.76 m/s. The interstitial fluid velocity must be high enough to lift the particles in the spout. If the calculated interstitial fluid velocity is greater than 15.76 m/s, the particles will start to move upwards. In Figure 6.16, the particles start to move upward at the minimum superficial gas velocity u_{ms} = 1.25 m/s, which yields an interstitial velocity of 18.75 m/s at the vessel bottom. Figure 6.17 shows the height-averaged vertical fluid velocity over the dimensionless heights (z/R_d) 14.164 - 25.218 in the downcomer for various inlet superficial gas velocities. The spatial distribution of the height-averaged vertical fluid velocity is fairly uniform at all superficial gas velocities. The fluid velocities in the downcomer region generally decrease as the superficial gas velocity increases. This may be ascribed to the fact that slugs occurring in the spout at low superficial gas velocities causes the flow resistance in the spout region to increase. This in turn causes the gas flow into the downcomer to relatively increase, compared to the case of a higher superficial gas velocity. As shown in Figure 6.17, the vertical fluid velocities near the draft plates and the walls are higher than elsewhere because the void fractions of the fluid cells close to them are slightly higher than elsewhere because of the channeling effect.

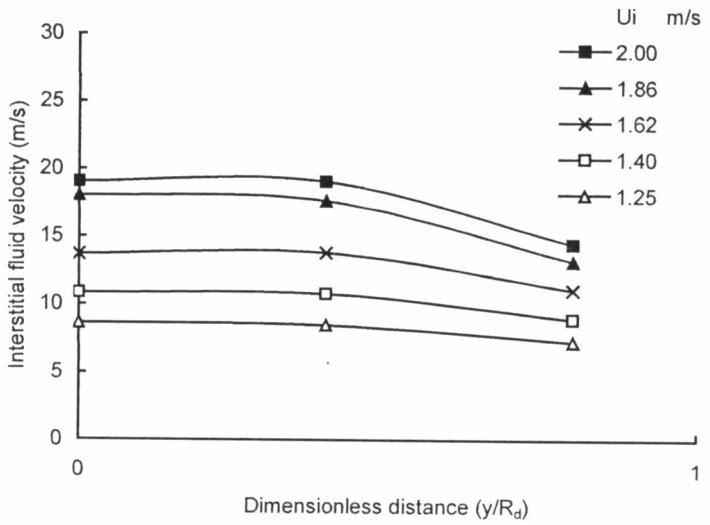

Figure 6.16 Profile of the height-averaged interstitial vertical fluid velocity profile over the dimensionless height (z / R_d) 14.164 – 25.218 in the spout region at various superficial gas velocities

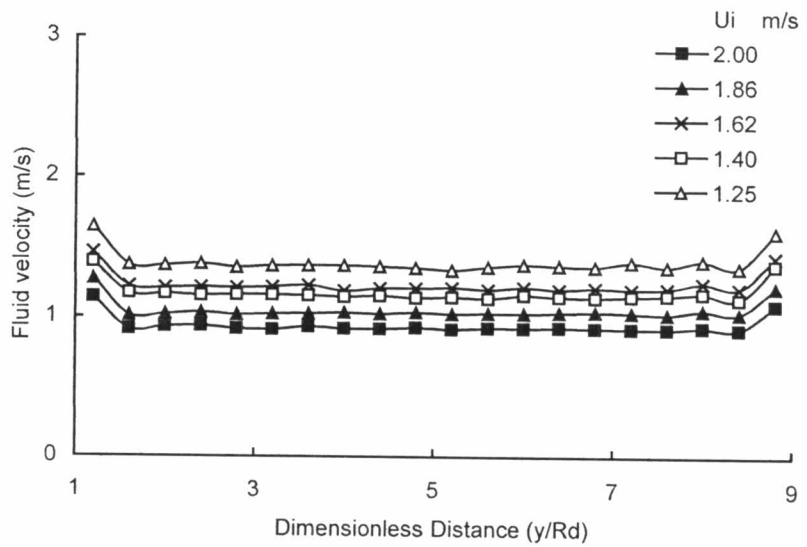

Figure 6.17 Profile of height-averaged vertical fluid velocity over the dimensionless heights (z/R_d) 14.164 - 25.218 in the downcomer for various inlet superficial gas velocities

6.1.2.5 Circulation rate of the particles

The particle circulation rate can be estimated from the particle velocity above slanting base, voidage, particle density and cross-sectional area of the downcomer as follows:

$$W_s = A_d v_p \rho_p (1-\varepsilon) \tag{6.4}$$

where W_s, A_d, v_p, ρ_p, ε are the particle circulation rate, cross-sectional area of the downcomer, particle velocity above the slanting base, particle density and voidage, respectively. As expected, the particle circulation rate increases with the increasing gas flow rate. As reported by Law-Kwet-Cheong (1986), a plot between the square root of the gas velocity and the particle circulation rate in Figure 6.18 yields a straight line.

6.2.1.5.1 Effect of separation height (H_e) on particle circulation rate

As mentioned above, Figure 6.18 shows an essentially linear relation between particle circulation rate and the square root of superficial gas velocity for both separation heights, 95 and 152 mm. When the separation height increases from 95 mm to 152 mm, the normal distance in Figure 6.1 increases from 37.97 mm to 66.47 mm, thus resulting in a larger number of particles entering the spout. The obtained empirical correlation for the particle circulation rate is as follows.

$$W_s = \begin{cases} 0.3251 u_i^{0.5} - 0.2652, & for\ He = 95\ mm \\ 0.1641 u_i^{0.5} + 0.1111, & for\ He = 152\ mm \end{cases} \tag{6.5}$$

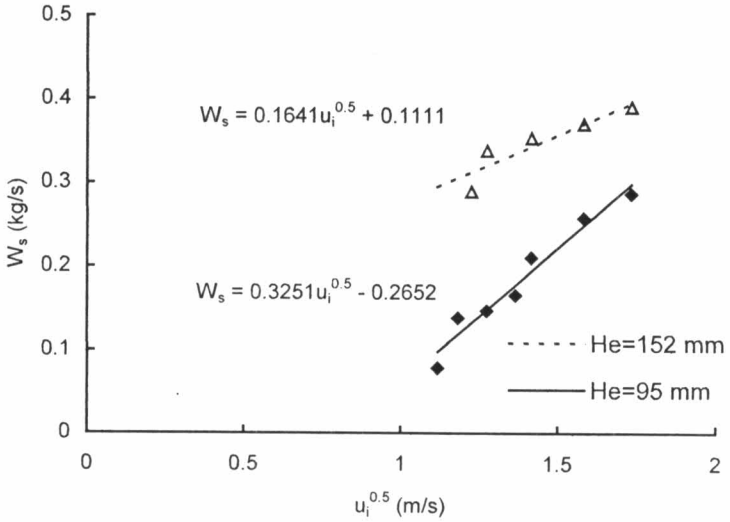

Figure 6.18 Relation between particle circulation rate and square root of superficial gas velocity (H_e= 95 mm, H_e= 152 mm)

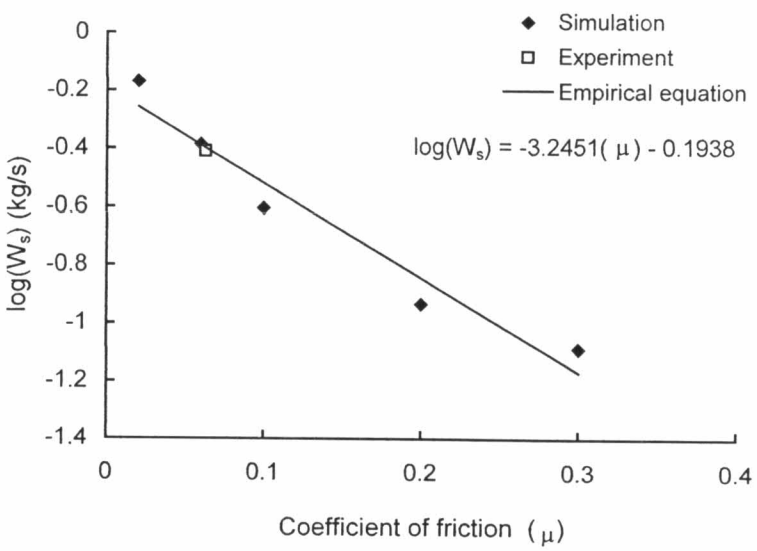

Figure 6.19 Relation between particle circulation rate and coefficient of friction at 1.25 m/s (u_{ms})

6.1.2.5.2 Effect of coefficient of friction on particle circulation rate

The calculated particle circulation rate at 1.25 m/s (= u_{ms}) as a function of the friction coefficient is shown in Figure 6.19. As expected, the particle circulation rate decreases as the friction coefficient increases. An apparent friction coefficient of 0.063 gives a circulation rate consistent with the experimental value of 0.39 kg/s reported by Kalwar (1991). Figure 6.19 reveals that the friction coefficient has a significant effect on the particle circulation rate in the 2DSB with draft plates. The obtained empirical equation for the circulation rate is as follows:

$$\log(W_s) = -3.245(\mu) - 0.1938 \tag{6.6}$$

where μ is the friction coefficient. As for the effect of the bed height, the simulation results at u_{ms} show that the bed height does not significantly affect the particle circulation rate in the 2DSB with draft plates, which is consistent with Kalwar (1991).

6.1.2.6 Effect of draft plates on the 2DSB

When the draft plates are removed from the vessel, our simulations show that spouting no longer occurs in the vessel at the bed height of 0.9 m (26,000 particles). A bubbling bed instead occurs in the vessel as shown in Figure 6.20. Even as the gas velocity is further increased, the bubbling bed still remains. The spouting does not occur in the vessel because the particle size is quite large. Malek and Lu (1964) found that the maximum spoutable bed depth decreased as the particle size increased. Figure 6.21 shows the observed flow patterns of the 2DSB at the bed height of 0.4 m (10,000 particles). Spouting does occur at this reduced bed height when the gas velocity sufficiently increases. The minimum spouting

velocity and pressure drop are about 2.0 m/s and 1.75 kPa, respectively. As expected, the minimum spouting velocity and pressure drop of the 2DSB without plates are higher than that with draft plates. It confirms that the draft plates can not only reduce the minimum spouting velocity and pressure drop but also increase the spoutable bed height.

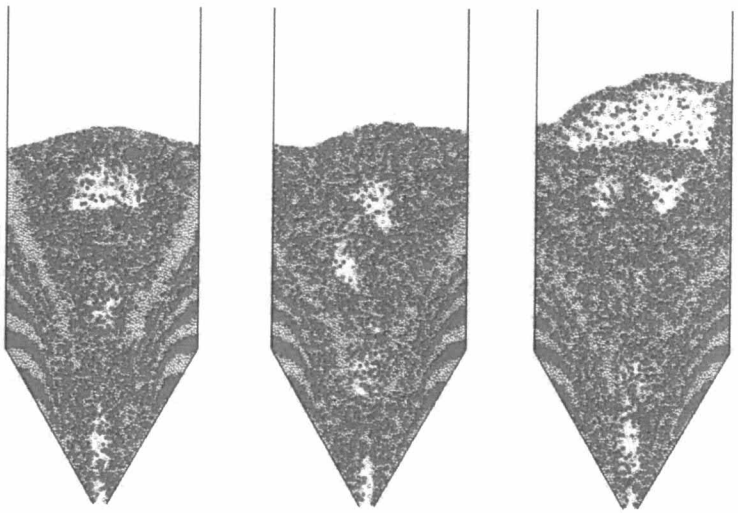

Figure 6.20 Flow patterns of 2DSBs at 26,000 particles

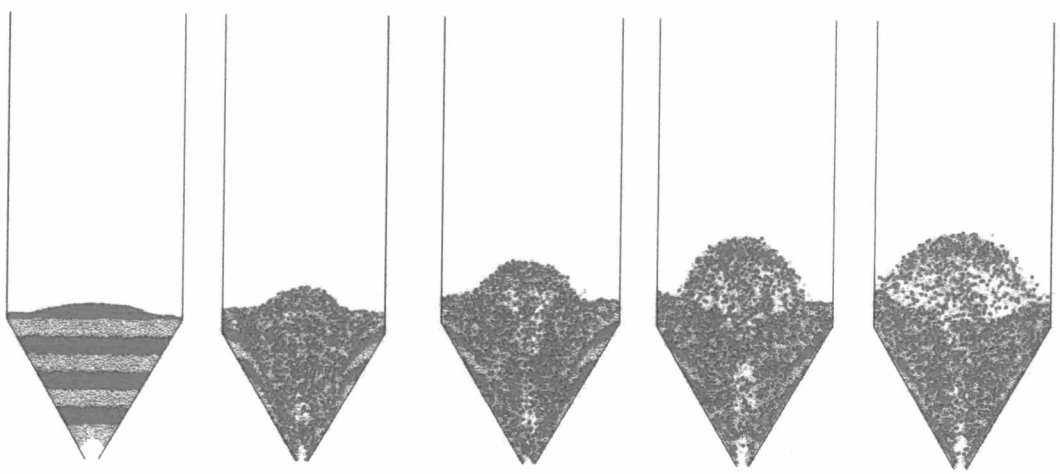

Figure 6.21 Flow patterns of 2DSBs at 10,000 particles

6.1.2.7 Effect of deflector in the 2DSB with draft plates

Generally, the deflector is installed in the 2DSB to prevent the unintentional entrainment of particles. On the minus side, an incorrectly installed deflector can induce breakage of particles. Kalwar (1991) reported that the optimally installed deflector is placed above the draft plates at a distance equal to 30% of the draft plate height (at 1.170 m). In the present work, we also investigate what would happen if a deflector were centrally located above the draft plates at a distance equal to 10%, 20% and 30% of the draft plate height. Figure 6.22 shows the calculated kinetic energy of the impacting particles averaged over a period of 4.5 seconds as a function of the location of the deflector and the superficial gas velocity. It is found that the kinetic energy upon impact decreases rapidly as the deflector height increases. The impacting kinetic energy at a superficial gas velocity of 1.62 m/s is highest because the slugs at this particular superficial velocity move with the highest average velocity. Beyond 1.62 m/s, the frequency of the slugs decreases and so does their average velocity as shown in Figure 6.3. Our simulation results reveal that the impacting kinetic energy at a distance equal to 30% of the draft plate height is sufficiently low to prevent breakage. The average kinetic energy and average velocity of the particles that collide at the deflector are 2.13×10^{-4} J and 0.97 m/s, respectively. This is consistent with the finding of Kalwar (1991).

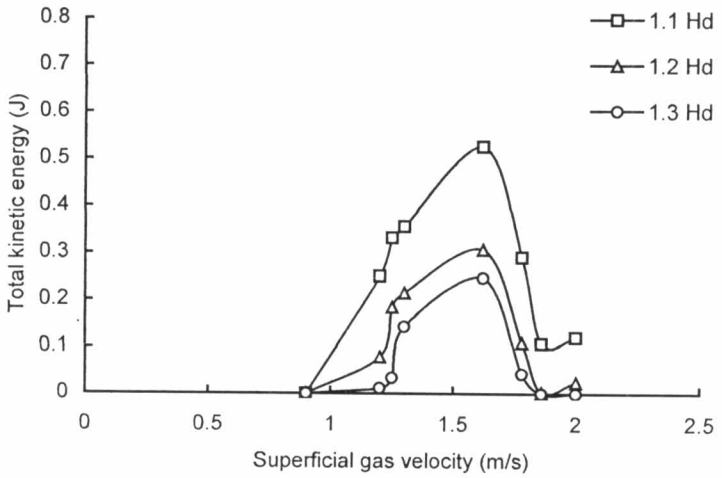

Figure 6.22 Total kinetic energy and superficial gas velocity

6.2 Effect of heat transfer on 2DSB with draft plates

When the hot gas is injected to the spouted bed at the bottom, gas-to-particle heat transfer occurs in the spouted bed. The phenomenon of gas-to-particle heat transfer is investigated in this work. Figure 6.23 and 6.24 show temperature profile of the particles in the spouted bed with draft plates at various times. It is found that gas-to-particle heat transfer occurs mainly in the central or spout region of the bed as the same reported by L.A.P Freitas and J.T. Freire (1998). Therefore, the particles will be heating in the spout region. The gas-to-particle heat transfer occurs mainly in the spout region because gas flow to the spout region is higher than that to the downcomer region. The temperature profile at the slanting base is lower than the other regions because friction between the particles and the slanting base retards the return flow of the particles to the spout. Figure 6.25,6.26 and 6.27 show the temperature profile of fluid in the spouted bed at various times. The fluid temperature in the spout region is higher than that in the downcomer region. The fluid temperature gradually increases until reach the steady state condition as shown in Figure 6.25,6.26 and 6.27.

Table 6.2 Conditions of simulation of heat transfer in 2DSB with draft plates

Parameter		Simulation
Particles		
Diameter, d_p	(m)	0.008
Density, ρ_p	(kg/m^3)	1,231
Spring constant	(N/m)	800
Coefficient of restitution		0.9
Coefficient of friction		0.3
Heat capacity	(J/kg K)	2,400
Sphericity, ϕ		1.0
Number of particles		26,000
Fluid		Properties of fluid at 338.8 K
Density	(kg/m^3)	1.043
Viscosity	(Pa s)	2.03×10^{-5}
Heat capacity	(J /kg K)	1,009
Thermal conductivity	(W/m K)	2.925×10^{-2}
Ambient fluid temperature	(K)	306.2
Inlet fluid temperature	(K)	423.2
Superficial fluid velocity	(m/s)	2.0

Table 6.3 Dimension of vessel for heat transfer in 2DSB with draft plates

Vessel		
Width, W	(m)	0.495
Depth, Lb	(m)	0.04
Width of gas inlet, Wi	(m)	0.033
Width of draft plates, Wd	(m)	0.055
Separation height, He	(m)	0.095
Spout height, Hd	(m)	0.912
Normal distance	(m)	0.03797
Slant angle, θ		60

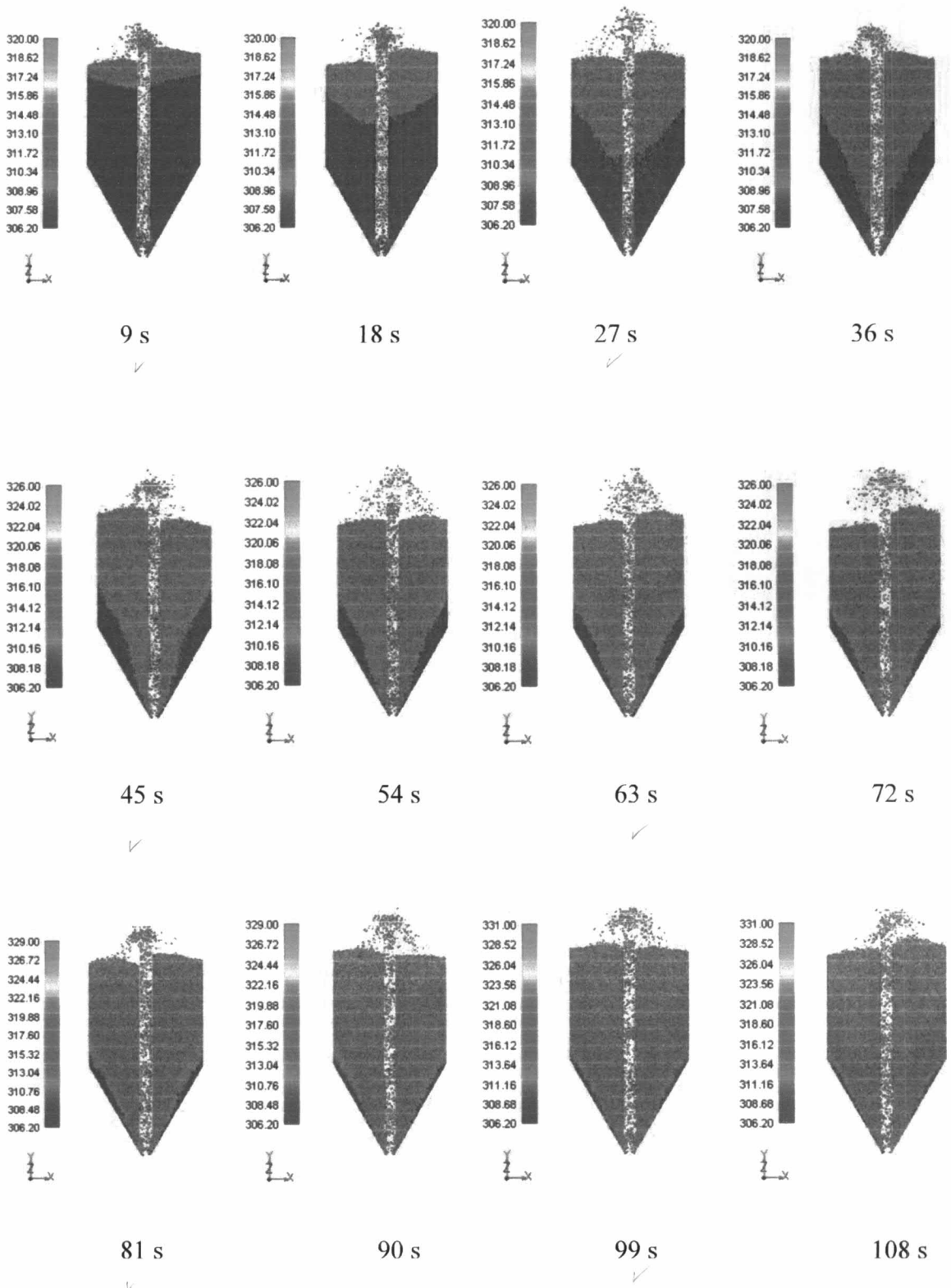

Figure 6.23 Profile of particle temperature in 2DSB at time 9 – 108 seconds

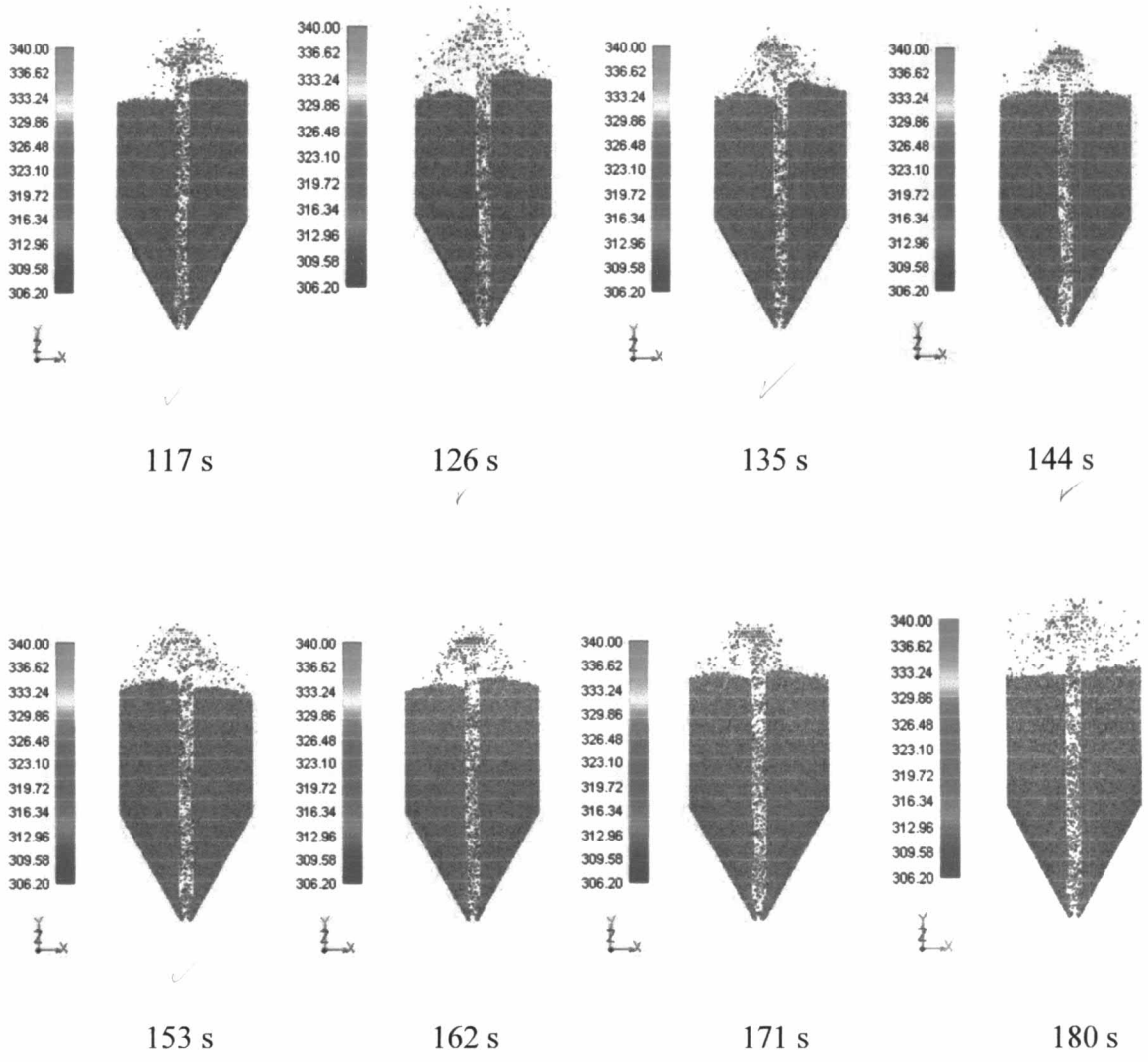

Figure 6.24 Profile of particle temperature in 2DSB at time 117 – 180 seconds

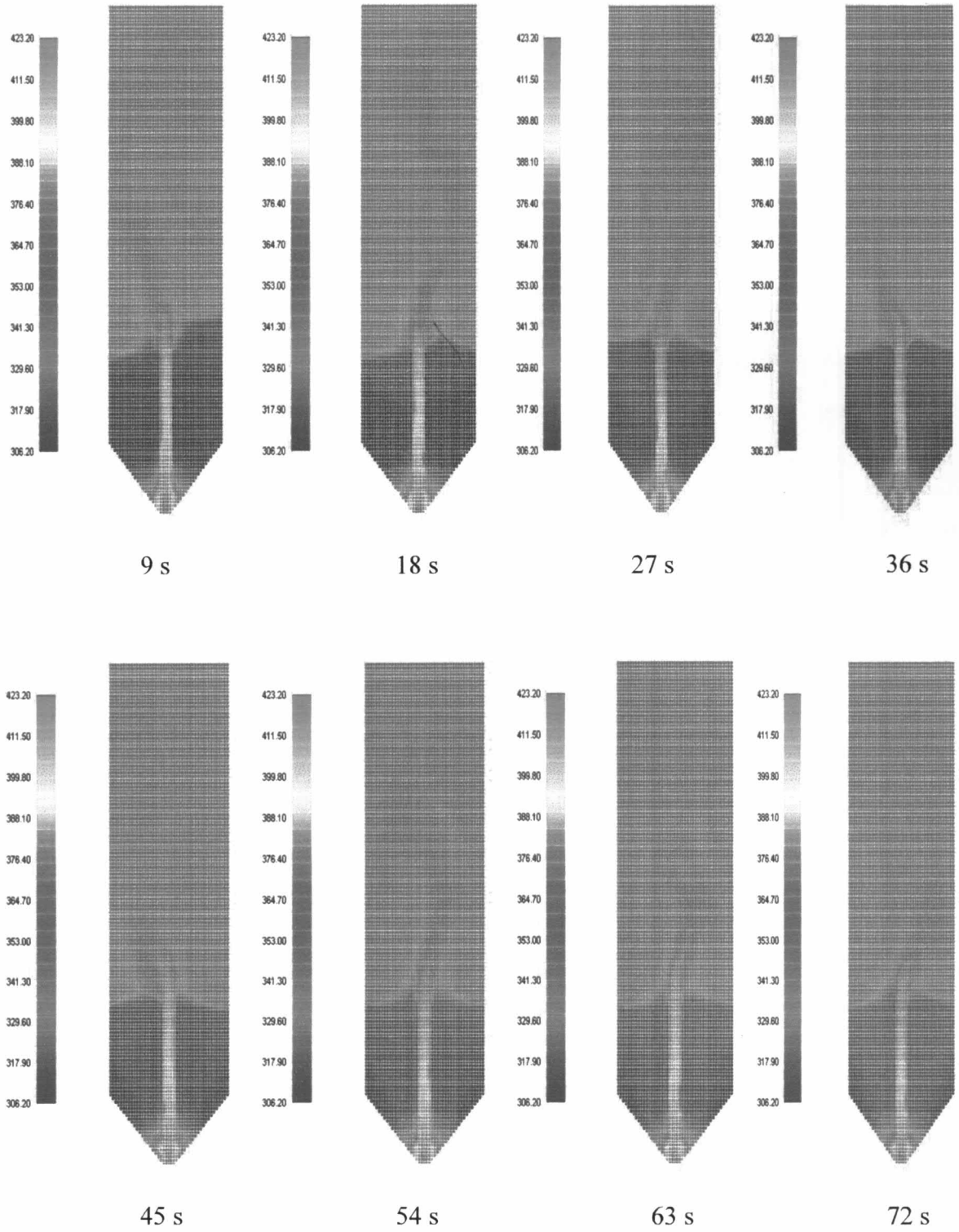

Figure 6.25 Profile of fluid temperature in 2DSB at time 9 – 72 seconds

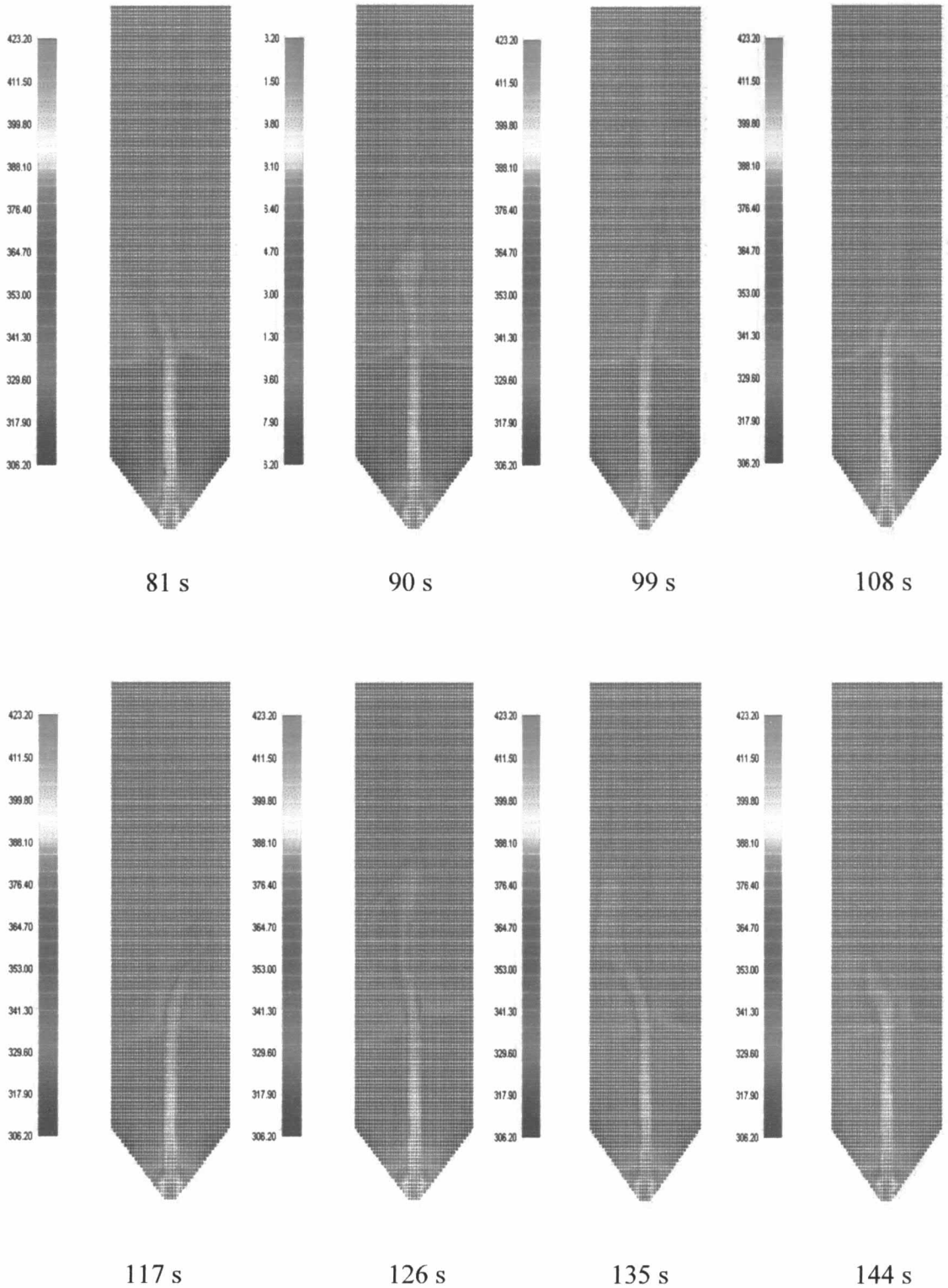

Figure 6.26 Profile of fluid temperature in 2DSB at time 81 – 144 seconds

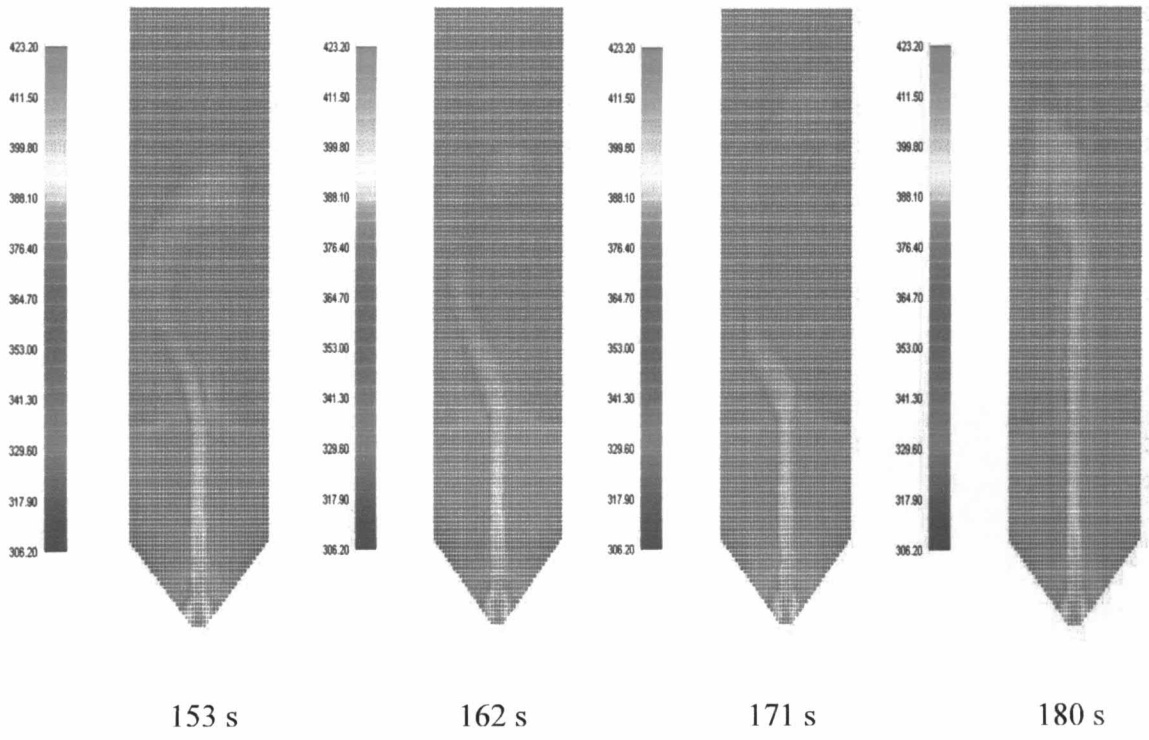

Figure 6.27 Profile of fluid temperature in 2DSB at time 153 – 180 seconds